Available online at www.sciencedirect.com
SCIENCE DIRECT®
Organic Electronics 4 (2003) 123–130
Organic Electronics
www.elsevier.com/locate/orgel

Tuning the performance of hybrid organic/inorganic quantum dot light-emitting devices

Seth Coe-Sullivan [a,1], Wing-Keung Woo [b,1], Jonathan S. Steckel [b], Moungi Bawendi [b], Vladimir Bulović [a,*]

[a] *Laboratory of Organic Optoelectronics, Department of Electrical Engineering and Computer Science, Massachusetts Institute of Technology, Cambridge, MA 02139, USA*
[b] *Department of Chemistry, Massachusetts Institute of Technology, Cambridge, MA 02139, USA*

Abstract

The luminescence of inorganic core-shell semiconductor nanocrystal quantum dots (QDs) can be tuned across much of the visible spectrum by changing the size of the QDs while preserving a spectral full width at half maximum (FWHM) as narrow as 30 nm and photoluminescence efficiency of 50% [Journal of Physical Chemistry B 101 (46) (1997) 9463] [1]. Organic capping groups, surrounding the QD lumophores, facilitate processing in organic solvents and their incorporation into organic thin film light-emitting device (LED) structures [Nature 370 (6488) (1994) 354] [2]. A recent study has shown that hybrid organic/inorganic QD-LEDs can indeed be fabricated with high brightness and small spectral FWHM, utilizing a phase segregation process which self-assembles CdSe(ZnS) core(shell) QDs onto an organic thin film surface [Nature 420 (6917) (2002) 800] [3]. We now demonstrate that the phase segregation process can be generally applied to the fabrication of QD-LEDs containing a wide range of CdSe particle sizes and ZnS overcoating thicknesses. By varying the QD core diameter from 32 Å to 58 Å, we show that peak electroluminescence is tuned from 540 nm to 635 nm. Increase in the QD shell thickness to 2.5 monolayers (~0.5 nm) improves the LED external quantum efficiency, consistent with a Förster energy transfer mechanism of generating QD excited states. In this work we also identify the challenges in designing devices with very thin (~5 nm thick) emissive layers [Chemical Physics Letters 178 (5–6) (1991) 488] [4], emphasizing the increased need for precise exciton confinement. In both QD-LEDs and archetypical all-organic LEDs with thin emissive layers, we show that there is an increase in the exciton recombination region width as the drive current density is increased. Overall, our study demonstrates that integration of QDs into organic LEDs has the potential to enhance the performance of thin film light emitters, and promises to be a rich field of scientific endeavor.

1. Motivation

Organic light-emitting devices (OLEDs) have been identified as a dominant new technology poised to realize the next generation of flat panel displays. OLED performance is exemplified by wide viewing angles, high color contrast, and low power consumption as compared to emissive liquid crystal displays [5]. Indeed, internal quantum efficiencies can approach 100% when organic phosphorescent molecules are used as the emitting materials [6]. A significant challenge of today's OLED technology remains the identification and

* Corresponding author.
E-mail address: bulovic@mit.edu (V. Bulović).
[1] These authors contributed equally to this work.

1566-1199/$ - see front matter
doi:10.1016/j.orgel.2003.08.016

synthesis of organic lumophores compatible with electrically pumped device structures [7]. Only a handful of efficient and long-lived organic phosphors have been incorporated into laboratory devices, while the ongoing research is aimed at the chemical design of new molecules, especially in the blue part of the spectrum [8]. As such, inorganic quantum dots (QDs) have generated interest in the OLED community as efficient alternative lumophores, whose saturated color emission can be tuned across the visible spectrum.

1.1. Quantum dots as lumophores

Inorganic semiconductor QDs are nanocrystals that are smaller in size than the diameter of a Bohr exciton in a bulk crystal of the same material. By reducing the size of the nanocrystal core, the quantum confinement of the QD electron, hole, and exciton is increased, with a consequent increase in the exciton energy. In CdSe nanocrystals, quantum confinement increases the exciton energy from a bulk bandgap of 1.7 eV (corresponding to wavelength, $\lambda = 730$ nm and the red edge of the visible spectrum) to any value up to 2.75 eV (corresponding to $\lambda = 450$ nm and blue luminescence).

The CdSe cores can be chemically synthesized with a surrounding shell of a wider band-gap semiconductor that passivates the surface states of the nanocrystal (see Fig. 1 inset), with a consequent increase in the QD photoluminescence quantum efficiency (η_{PL}). For example, η_{PL} of

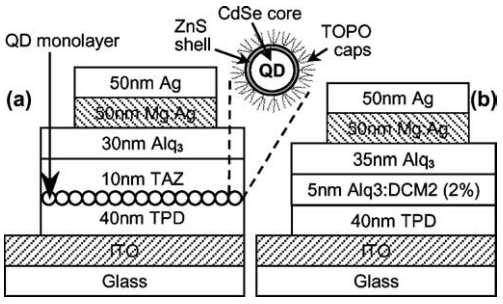

Fig. 1. Device cross-sections of the two LEDs discussed in the paper. (a) QD-LED structure. (b) Model DCM2 doped OLED structure. Inset depicts CdSe(ZnS) core-shell-cap QD structure.

CdSe QDs can increase from below 20% for bare QDs in solution to 50% for QDs overcoated with several monolayers of ZnS [1]. To achieve a narrow QD luminescence spectrum, the size distribution of CdSe(ZnS) QDs in a solution sample can be narrowed through selective precipitation to have a standard deviation of 5–8% in diameter [9], which translates to a spectral full width at half of maximum (FWHM) in solution of <30 nm.

Finally, solution processing of inorganic nanocrystals is facilitated by the organic capping groups that dress the surface of the QDs. The capping layer may be tailored to control solubility, external chemistry, and particle spacing in a QD thin film. All of these independent controls make for a versatile material set for the creation of lumophores that could be imbedded within organic LEDs. The purpose of this work is to explore the full range of nanocrystal properties that affect the performance of QD-LEDs.

1.2. Historical perspective

The first published work on LEDs incorporating colloidally grown CdSe QDs [2] was a bilayer device utilizing a polymer hole transporting layer, and a 15–25 nm thick QD film (5 QD monolayers of 3–5 nm diameter) as the electron transporting layer. Contemporaneously, a QD-LED structure was fabricated incorporating QDs within a semiconducting polymer matrix [10]. While the external electroluminescence (EL) quantum efficiency reported in both papers was low ($\eta_{EL} < 0.01\%$), the studies demonstrated that electrically generated QD EL was possible, alluding to the technological potential of QD-LEDs. Subsequent papers explored the benefits of combining these two approaches [11], as well as the use of overcoated CdSe(ZnS) [12] and CdSe(CdS) QDs [13]. Development of these devices yielded η_{EL} as high as 0.22% [13] but with response times in excess of several seconds. A new QD material set, InAs(ZnSe), was recently used to generate efficient EL in the near infrared [14]. This was followed by our demonstration of $\eta_{EL} = 0.5\%$ visible QD-LEDs that incorporate a single layer of QDs in a molecular organic structure [3], and the present study extends upon this to yield $\eta_{EL} = 1.1\%$. The

fast response time and higher η_{EL} of these latest devices matches that of fluorescent OLEDs.

In our previous studies highly engineered QD-LEDs demonstrated high performance and narrowband EL spectra, primarily from QD emission [3]. Achieving an optimized device required repeated experimentation due to the variation of QD sample size distribution, PL efficiency, and solution concentration. The limited quantity of QDs produced per batch (<100 mg) requires reoptimization for each new sample. In the present study we have not fully optimized the performance of each of the shown devices, and instead have focused on deciphering the details of QD-LED operation. Indeed, in a manufacturing process, with large batch synthesis and good quality control, such reoptimization should not be necessary.

2. Experimental

Our basic QD-LED structure is shown in Fig. 1(a). The bilayer film is first deposited from a solution of *N*, *N*′-diphenyl-*N*, *N*′-bis(3-methylphenyl)-(1, 1′-biphenyl)-4, 4′-diamine (TPD) and QDs in chloroform ($CHCl_3$) that is spin coated (Headway Research, PWM32-PS-R790 Spinner System) onto a cleaned ITO coated glass substrate [3]. Phase segregation occurs as the solvent dries during this process forming the TPD/QD (40 nm total thickness) bilayer. The relative amount of TPD can be varied to control the TPD layer thickness, and the QD concentration in solution is used to optimize the QD monolayer coverage. Profilometry (Tencor, P10 Surface Profiler) and atomic force microscopy (Digital Instruments, Nanoscope IIIa, tapping mode, Silicon probe tip) are used to inspect QD and TPD thickness and morphology. Fig. 2 shows examples of TPD/QD bilayer films in which the TPD film surface is covered with different amounts of QDs. The QD coverage can be tailored reliably from low (<25%) coverages, Fig. 2(a), all the way to 100% coverage for monodisperse samples, Fig. 2(e). A 10 nm thick film of 3-(4-Biphenylyl)-4-phenyl-5-tert-butylphenyl-1, 2, 4-triazole (TAZ) is then thermally evaporated over the entire substrate area, followed by a 30 nm thick tris-(8-hydroxyquinoline) aluminum (Alq_3) film. Finally, an evaporated Mg:Ag/Ag electrode (50:1 Mg:Ag by weight) is patterned on top using a contact shadow mask. We note that in some devices the TAZ layer has been omitted, as indicated in the text. The spin-on deposition is done within a controlled nitrogen environment (<5 ppm O_2, H_2O), and the evaporator base pressure is 5×10^{-8} Torr. It is our experience that exposure to atmospheric conditions can strongly influence the quality of the deposited films, manifested as both reduced EL efficiency and morphological changes. Thus, the QD-LEDs of the present study are not exposed to air until testing, when the top electrode acts as a temporary encapsulation to the underlying active layers. For a series of devices, EL color is controlled entirely by changing the QD diameter.

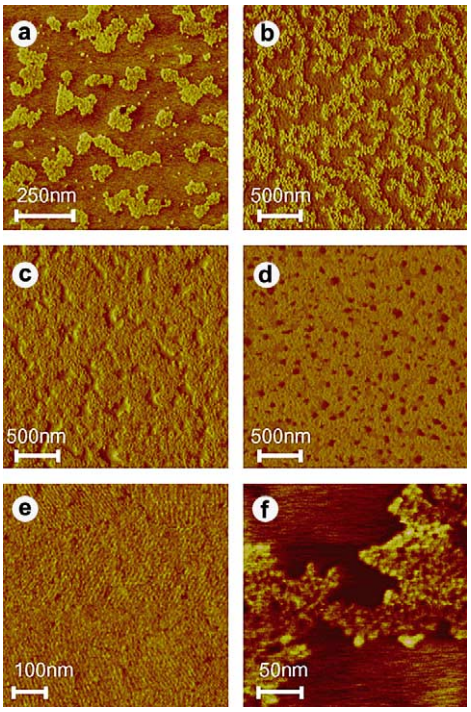

Fig. 2. Atomic force microscopy (AFM) images showing various coverage fractions of a QD monolayer (yellow) on a smooth TPD film (red). (a) QD monolayer coverage is 20%, (b) 50%, (c) 80%, (d) 90%, (e) 100%. (f) Result of spinning a bilayer TPD/QD film from a QD sample with large size distribution. Disordered clusters of QDs are formed.

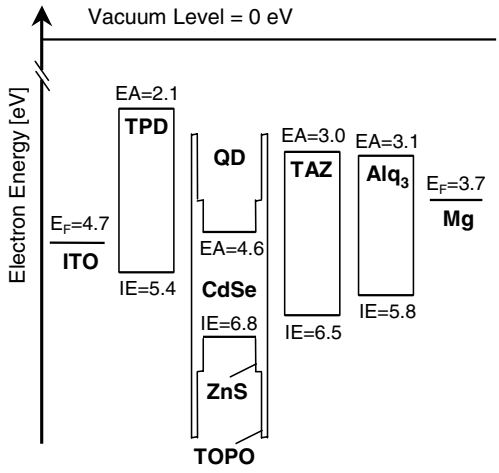

Fig. 3. Energy diagram for QD-LEDs of Fig. 1(a). The highest occupied molecular orbital (HOMO) and lowest unoccupied molecular orbital (LUMO) band energies were determined from photoemission spectroscopy and inverse photoemission spectroscopy measurements [20], while the QD energy structure has been calculated [12].

3. Results and analysis

3.1. Electroluminescence

Fig. 3 shows the band structure for the device of Fig. 1(a). Increase in the QD band gap (0.3 eV over the demonstrated tuning range of this study) will have minimal impact on the relative alignment of energy levels. For devices which include the TAZ exciton blocking layer, an additional emission peak corresponding to TPD EL is observed. Devices without the TAZ layer have an additional emission peak at 530 nm, identified as Alq_3 EL.

Fig. 4(a) shows the EL spectra of different QD-LEDs operated at low current density (0.38–13 mA/cm^2, Fig. 4(a)). The spectra demonstrate our ability to fabricate devices which yield highly monochromatic EL that is tunable from 540 to 635 nm, corresponding to the PL spectrum of each QD starting solution. The EL of these devices has greater than 70% QD emission. The remaining organic (Alq_3 or TPD) EL is due to the presence of voids, grain boundaries, and interstitial spaces in the QD monolayers that allow the creation of excitons on organic sites as depicted in Fig. 5. For example, excitons generated in region A, deep within the electron transporting layer, are more than the Förster energy transfer radius (R_F) away from the nearest QD, resulting in organic EL. Similarly, excitons in region B, within the monolayer void, will result in organic EL.

Fig. 4(b) shows the EL spectra of QD-LEDs operated at higher current density (130 mA/cm^2). Comparing to Fig. 4(a), it is clear that the fraction of emission coming from organic lumophores has increased. Fig. 4(c) demonstrates this same effect for a single QD-LED operated over 3 decades of current densities, from 0.38 to 380 mA/cm^2. This change in ratio of QD to organic EL signifies a notable change in the exciton generation process.

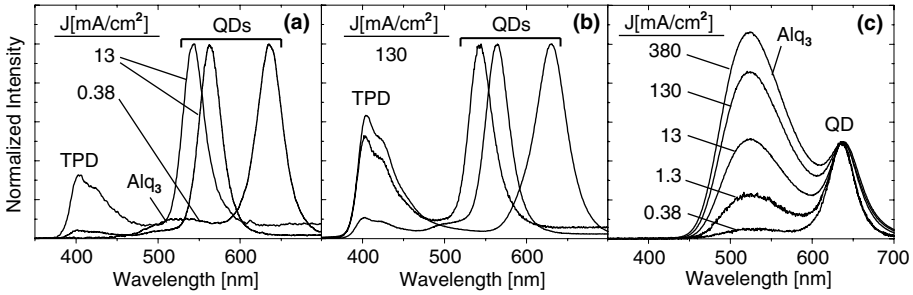

Fig. 4. Typical normalized QD-LED electroluminescence spectra of three different sized QD samples measured at (a) low current levels (0.38–13 mA/cm^2), where most (>70% in all cases) of the emission is from the QDs in the device, with only small spectral contributions from either Alq_3 (when TAZ layer is omitted) or TPD (when TAZ layer is present) (b) moderate current levels (130 mA/cm^2), where two of the three spectra have a large fraction of EL from TPD (c) and a progression of currents for a single device (from 0.38 to 380 mA/cm^2). Note that the devices emitting at 540 and 560 nm are the same in 4(a) and 4(b). At low currents, a larger portion of the excitons are created within a Förster energy transfer radius of the QD monolayer. For all devices, $0.2\% < \eta_{EL} < 0.5\%$.

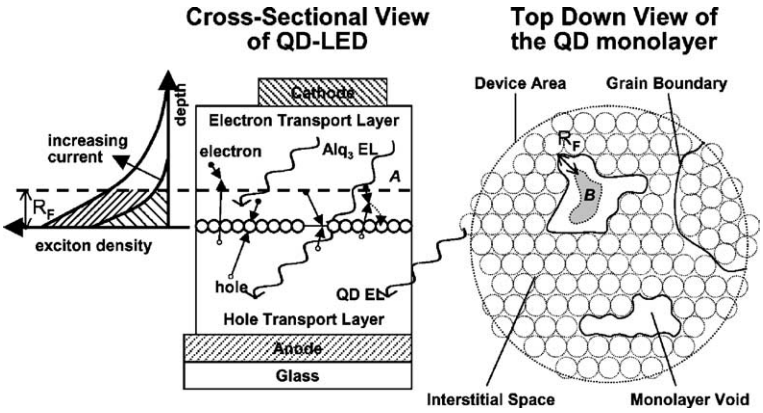

Fig. 5. Graphic representation of exciton generation process within the QD-LED structure. At high currents the width of the exciton generation region is expected to exceed the organic-QD Förster energy transfer radius (R_F) (region A in the figure), resulting in an increased contribution of organic (Alq_3 or TPD) luminescence to the EL spectrum. Excitons created at voids (region B in the figure), interstitial spaces and grain boundaries of the QD monolayer may also be farther than R_F away from the nearest QD.

In the previous study [3] we noted that EL is generated by either direct injection of holes and electrons into the QDs or by the Förster energy transfer of excitons onto the QDs from the neighboring organic molecules of higher exciton energy (note that the PL of TPD and Alq_3 overlaps with the absorption spectra of all QDs in this study). In the energy transfer picture we can attribute the organic emission to the recombination of excitons in the organic molecules which are at a distance $> R_F$ from the nearest QD. Therefore, at lower currents, either all excitons have energy transferred from organic molecules to QDs, or alternatively, they are initially formed by direct charge injection on the QD sites. We note that at the current density of 130 mA/cm^2, at most 10^6 electrons per second arrive at each QD site so that the rapid QD exciton relaxation (thin film CdSe QD exciton lifetime $\tau_{QD} < 10$ ns [15]) keeps the QD exciton density at <1%. Such a low QD exciton population should not modify the organic-QD exciton transfer rate, and consequently the change in the QD emission fraction with current could be due to a change in the exciton recombination region width.

Following an earlier study [16] we suggest that the exciton recombination region of QD-LEDs broadens with increasing current, which we confirm by using an archetype OLED system, DCM2 doped into a TPD/Alq_3 structure. The OLED cross-section is shown in Fig. 1(b), with the red laser dye DCM2 used in place of QDs. The dye is doped at low concentration (2% by weight) in a 5 nm thick Alq_3 layer, to closely model the thin two-dimensional QD sheet that makes up the emissive layer of the QD-LED structures. With this device we can study the performance of a very thin and extensively characterized lumophore layer, eliminating QDs as a performance modifier. The spectral dependence on current density is then measured over 4 decades of current. From the normalized EL spectra in Fig. 6 it is clear that the ratio of Alq_3 to DCM2 emission rises with increasing current density. The observed changes in Fig. 6 are consistent with the spectral changes of the QD-LED in Fig. 4(c). Equivalently, the organic emission in the QD devices is a consequence of the very thin QD lumophore layer, suggesting the need for better confinement of excitons near the QDs. To date, however, fabrication of an effective exciton confinement structure has been complicated by the difficulty in depositing a uniform thin (<10 nm) aromatic film on top of an alkane capped QD monolayer, as morphological studies have explored [3].

3.2. Effect of the QD core diameter on QD-LED performance

For the most efficient operation of QD-LEDs, it is desirable to have QDs with high η_{PL} and large

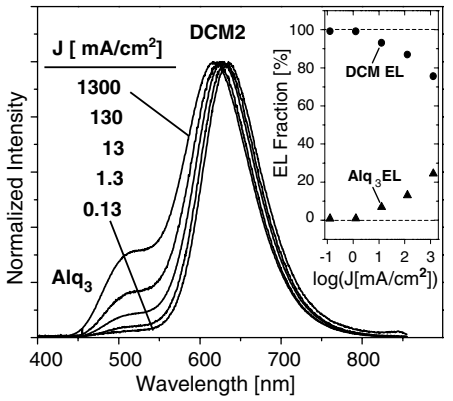

Fig. 6. Normalized electroluminescence spectra from the DCM2 doped OLED shown in Fig. 1(b). The five curves are at five different current levels, each an order of magnitude higher than the previous. At the lowest current density (0.13 mA/cm^2) the device is nearly monochromatic, emitting only from DCM2 sites. As the current is increased, a larger fraction of the emission is from the Alq_3 sites. Inset is a plot of emission fraction versus current density for Alq_3 and DCM2 EL.

absorption cross-section, maximizing R_F of the energy transfer from organic molecules to QDs. High η_{PL} is in general easier to achieve for larger diameter QD samples. As the absorption cross-section is greatly increased for larger QDs, large QDs would seem to be the ideal lumophore for QD-LEDs. However, QD sample size distributions are more difficult to control for larger diameter QDs. The close packing of QDs on top of organic films was improved for QD solution samples with a narrow distribution of QD sizes (Fig. 2(e)), as reflected in their narrow (30 nm FWHM) PL spectra. QD samples with a large standard deviation of size distribution typically formed disordered films as in Fig. 2(f).

Considering the above dependence of size distribution, η_{PL}, and absorption cross-section on the QD diameter, high color purity, high efficiency devices are easiest to generate in the middle of the CdSe QD size range, near 560 nm. Other semiconductors, such as ZnSe or CdTe, can be used to access the extremes of blue and red emission, respectively. Such changes to the core semiconductor material can be made without modifying the chemical nature of the capping groups, leaving the device fabrication process unchanged.

3.3. Effect of QD overcoating thickness on QD-LED performance

The η_{PL} of a QD sample increases with the thickness of the overcoating layer for the first 2.5 monolayers of ZnS ($\sim$0.5 nm). For a bare QD (or zero overcoating thickness) the η_{PL} is in general lower than for an overcoated sample due to unpassivated surface quenching sites. However, overcoating increases the total diameter of a QD, thus making it more difficult to maintain the size distribution of an overcoated QD sample. For this reason, as well as concerns that higher overcoating thicknesses would hurt energy delivery into the QD core, most of the QD-LEDs in this study have 0.7 ± 0.2 monolayer overcoated QDs (Figs. 2 and 4).

However, we did fabricate a QD-LED incorporating CdSe(2.5 ZnS monolayers) QDs. EL efficiency, emission spectra, and current–voltage characteristics of this device are compared to the performance of a QD-LED incorporating CdSe(0.7 ZnS monolayers). In the preparation of both overcoating thicknesses, the same 58 Å diameter CdSe core QDs are used. In Fig. 7, η_{EL} is observed to increase by a factor of three, to $\eta_{EL} = 1.1\%$, which is comparable to the increase in η_{PL} of the two QD solutions. However, we note that creating such a device is more difficult experimentally than creating a device out of thinly overcoated QDs, due to the broadening of size distribution that is frequently associated with 2.5 monolayer overcoated QDs. Further optimization of the spun-on QD monolayer coverage should yield a monochrome device, emitting only at 635 nm. Since the η_{EL} of the best TPD/TAZ/Alq_3 device fabricated in our laboratory is 1.0%, we conclude that the η_{EL} for a perfectly monochromatic QD-LED should be in excess of 1.1%.

If the mechanism of exciton creation were direct charge injection into QDs, then the increase in tunnel barrier thickness for thicker overcoatings would correspond to a tenfold decrease in hole injection into the QD (calculated using WKB approximation, relying on the band diagram in Fig. 3). In contrast, the only tunnel barrier to electron injection from Alq_3 to QDs is in the monolayer thin TOPO cap. Such change in the ratio of hole

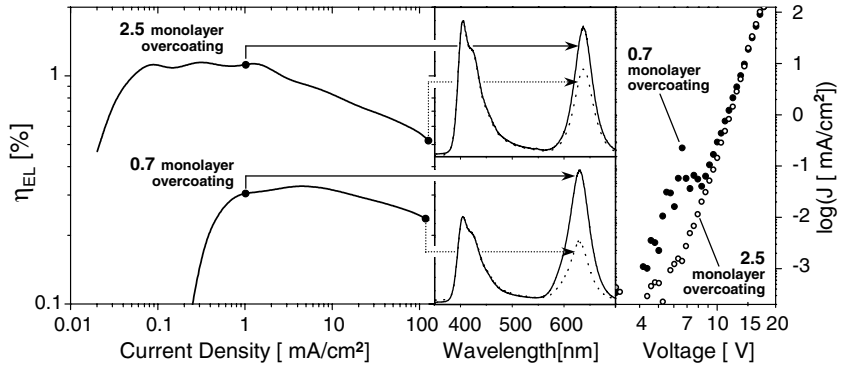

Fig. 7. The external quantum efficiency (peak $\eta_{EL} = 1.1\%$) for a magenta emitting QD-LED utilizing 2.5 ZnS monolayers overcoated QDs is compared to a QD-LED incorporating 0.7 ZnS monolayer overcoated QDs. In both devices, roughly half of the emission is from the TPD hole transporting layer and increases with increasing current. The current–voltage characteristics for the two devices are almost identical, demonstrating that the thicker overcoated, single monolayer of QDs has minimal influence on charge conduction. For the 2.5 ZnS monolayer overcoated QDs, the η_{EL} of the device goes up, despite the thicker tunnel barrier that the holes need to penetrate for direct charge injection.

and electron injection into the QDs with overcoating thickness would be reflected as a significant change in the η_{EL} measured in these two devices. Since the η_{PL} increase completely describes the change in observed η_{EL} we conclude that direct charge injection is not the dominant mechanism of exciton creation on the QDs. Instead, we propose that Förster energy transfer of excitons from organic host material to the QDs dominates the EL process. The 0.5 nm increase in ZnS shell thickness is much smaller than the expected Förster radius and hence should have minimal effect on the Förster transfer rate [17].

4. Perspective

Based on the present study we can ascertain the shortcomings of the two major categories of devices fabricated prior to 2002. For devices in which QDs were homogeneously distributed in a polymer matrix, we expect that the QDs were strongly influencing the film morphology and charge conduction through the polymer layer. Rough surface morphology, typical of thick (more than a few monolayers) QD films likely contributed to the observed low device yields and allowed little freedom in optimizing charge injection, transport and position of the exciton recombination region. In the devices in which QDs were deposited as thick, neat films, the QDs functioned as both lumophores and charge transport layers. QD photoconductivity experiments give us direct evidence of the poor conduction properties of thick QD films relative to organic semiconductors [18]. In addition, thin films that have both charge and excitons present often undergo quenching mechanisms such as polaron–exciton quenching or Auger recombination [19]. In our most recent work, using a self-assembled single monolayer of QDs, sandwiched between two thin films of molecular organic semiconductors, the QDs function exclusively as lumophores. The result is devices that are both more efficient, and easier to optimize.

QD-LEDs are a verastile test-bed for studying the electrical and optical behavior of QDs in the solid state. Active devices allow us to probe the electrical properties of single monolayers of QD solids. Furthermore, there is evidence that such devices could satisfy the technological requirements of flat panel displays and imaging applications which require the narrowband emission characteristic of QDs, as well as the efficient creation of visible light in the blue and red regions of the spectrum. In a span of eight years QD-LED efficiency has improved over two orders of magnitude reaching the luminous and quantum efficiencies of fluorescent OLEDs. This rapid advance

was facilitated by the expanding knowledge of the OLED community whose developments are largely applicable to the QD-LED structures. Indeed, we identify QD-LEDs as a kin technology to OLEDs, potentially complementing their performance when highly saturated color emission is desirable. It is conceivable that with further development, QD-LEDs could reach the efficiencies of phosphorescent OLEDs through incorporation of QDs in organic triplet generating hosts. The combination of inorganic luminescent properties, with the advantages of organic processing techniques, suggest the possibility of creating robust, large area emitters with physical properties that are tailored on the nanoscale. The present pursuit of QD-LEDs has the potential for near term scientific and technological impact, as the fabrication and synthetic processes are perfected.

Acknowledgements

This research was funded in part by the NSF-MRSEC program, DMR, and Universal Display Corporation. This work made use of MRSEC Shared Facilities supported by the National Science Foundation.

References

[1] B.O. Dabbousi et al., (CdSe)ZnS core-shell quantum dots: synthesis and characterization of a size series of highly luminescent nanocrystallites, Journal of Physical Chemistry B 101 (46) (1997) 9463–9475.
[2] V.L. Colvin, M.C. Schlamp, A.P. Alivisatos, Light-emitting-diodes made from cadmium selenide nanocrystals and a semiconducting polymer, Nature 370 (6488) (1994) 354–357.
[3] S. Coe et al., Electroluminescence from single monolayers of nanocrystals in molecular organic devices, Nature 420 (6917) (2002) 800–803.
[4] M. Era et al., Double-heterostructure electroluminescent device with cyanine-dye bimolecular layer as an emitter, Chemical Physics Letters 178 (5–6) (1991) 488–490.
[5] V. Bulovic, S.R. Forrest, Polymeric and molecular organic light emitting devices: A comparison, Electroluminescence Ii 65 (2000) 1–26.
[6] C. Adachi et al., Nearly 100% internal phosphorescence efficiency in an organic light-emitting device, Journal of Applied Physics 90 (10) (2001) 5048–5051.
[7] C. Adachi et al., High-efficiency red electrophosphorescence devices, Applied Physics Letters 78 (11) (2001) 1622–1624.
[8] S.K. Kwon et al., Novel blue organic light emitting materials, Molecular Crystals and Liquid Crystals 377 (2002) 19–23.
[9] C.B. Murray, C.R. Kagan, M.G. Bawendi, Synthesis and characterization of monodisperse nanocrystals and close-packed nanocrystal assemblies, Annual Review of Materials Science 30 (2000) 545–610.
[10] B.O. Dabbousi et al., Electroluminescence from CdSe quantum-dot polymer composites, Applied Physics Letters 66 (11) (1995) 1316–1318.
[11] H. Mattoussi et al., Composite thin films of CdSe nanocrystals and a surface passivating /electron transporting block copolymer: Correlations between film microstructure by transmission electron microscopy and electroluminescence, Journal of Applied Physics 86 (8) (1999) 4390–4399.
[12] H. Mattoussi et al., Electroluminescence from heterostructures of poly(phenylene vinylene) and inorganic CdSe nanocrystals, Journal of Applied Physics 83 (12) (1998) 7965–7974.
[13] M.C. Schlamp, X.G. Peng, A.P. Alivisatos, Improved efficiencies in light emitting diodes made with CdSe(CdS) core/shell type nanocrystals and a semiconducting polymer, Journal of Applied Physics 82 (11) (1997) 5837–5842.
[14] N. Tessler et al., Efficient near-infrared polymer nanocrystat light-emitting diodes, Science 295 (5559) (2002) 1506–1508.
[15] C.R. Kagan, C.B. Murray, M.G. Bawendi, Long-range resonance transfer of electronic excitations in close-packed CdSe quantum-dot solids, Physical Review B 54 (12) (1996) 8633–8643.
[16] V. Bulovic et al., Weak microcavity effects in organic light-emitting devices, Physical Review B 58 (7) (1998) 3730–3740.
[17] S.A. Crooker et al., Spectrally resolved dynamics of energy transfer in quantum-dot assemblies: Towards engineered energy flows in artificial materials, Physical Review Letters 89 (18) (2002), p. art. no.-186802.
[18] C.A. Leatherdale et al., Photoconductivity in CdSe quantum dot solids, Physical Review B 62 (4) (2000) 2669–2680.
[19] V.I. Klimov, D.W. McBranch, Femtosecond 1P-to-1S electron relaxation in strongly confined semiconductor nanocrystals, Physical Review Letters 80 (18) (1998) 4028–4031.
[20] I.G. Hill, A. Kahn, Organic semiconductor heterointerfaces containing bathocuproine, Journal of Applied Physics 86 (8) (1999) 4515–4519.